Published in final edited form as:
Magn Reson Imaging. 2015 January ; 33(1): 56–62. doi:10.1016/j.mri.2014.08.040.

Reduced-FOV Excitation Decreases Susceptibility Artifact in Diffusion-Weighted MRI with Endorectal Coil for Prostate Cancer Detection

Natalie Korn[1], **John Kurhanewicz, PhD**[1,2], **Suchandrima Banerjee, PhD**[3], **Olga Starobinets**[1,2], **Emine Saritas, PhD**[4], and **Susan Noworolski, PhD**[1,2]

[1]Department of Radiology and Biomedical Imaging, University of California at San Francisco, San Francisco, CA

[2]The Graduate Group in Bioengineering, University of California at San Francisco and Berkeley, San Francisco and Berkeley, CA

[3]General Electric Healthcare, Menlo Park, CA

[4]Department of Bioengineering, University of California at Berkeley

Abstract

The purpose of this study was to determine if image distortion is less in prostate MR apparent diffusion coefficient (ADC) maps generated from a reduced-field-of-view (rFOV) diffusion-weighted-imaging (DWI) technique than from a conventional DWI sequence (CONV), and to determine if the rFOV ADC tumor contrast is as high as or better than that of the CONV sequence. Fifty patients underwent a 3T MRI exam. CONV and rFOV (utilizing a 2D, echo-planar, rectangularly-selective RF pulse) sequences were acquired using b=600, 0 s/mm^2. Distortion was visually scored 0–4 by three independent observers and quantitatively measured using the difference in rectal wall curvature between the ADC maps and T2-weighted images. Distortion scores were lower with the rFOV sequence ($p<0.012$, Wilcoxon Signed-Rank Test, n=50), and difference in distortion scores did not differ significantly among observers ($p=0.99$, Kruskal-Wallis Rank Sum Test). The difference in rectal curvature was less with rFOV ADC maps (26±10%) than CONV ADC maps (34±13%) ($p<0.011$, student's t-test). In seventeen patients with untreated, biopsy confirmed prostate cancer, the rFOV sequence afforded significantly higher ADC tumor contrast (44.0%) than the CONV sequence (35.9%), ($p<0.0012$, student's t-test). The rFOV sequence yielded significantly decreased susceptibility artifact and significantly higher contrast between tumor and healthy tissue.

Corresponding Author: Natalie Korn, Department of Radiology and Biomedical Imaging, University of California at San Francisco, San Francisco, CA, The Graduate Group in Bioengineering, University of California at San Francisco and Berkeley, San Francisco and Berkeley, CA, The University of California, 185 Berry Street, Suite 350, Box 0946, San Francisco, CA 94107, FAX: 415-353-4847, Phone: 415-514-6790, Natalie.Korn@ucsf.edu.

Keywords

reduced FOV; prostate; diffusion-weighted imaging; MRI; endorectal; ADC

1. Introduction

Prostate cancer is the second most common type of cancer in the American male population [1]. Because prostate cancer shows a high incidence and low mortality rate in comparison with other cancers [1], an urgent need exists to develop non-invasive imaging approaches for improved prostate cancer patient-specific treatment planning and early assessment of therapeutic failure.

Multiparametric MRI has been studied extensively for identifying prostate cancer [2] through a combination of T2-weighted imaging, dynamic contrast-enhanced imaging, ^{1}H MR spectroscopy, and diffusion-weighted imaging (DWI). To further increase diagnostic capability, the multiparametric MRI can include the use of an endorectal coil in conjunction with a standard pelvic phased-array. Combining endorectal and phased-array coils has proven to increase the signal-to-noise ratio of DWI in prostate exams at 3T over nine times in comparison to use of a phased-array alone. [3].

DWI increases both sensitivity and specificity in prostate cancer detection in multiparametric MR studies [4–6]. DWI has also been shown to improve the assessment of tumor aggressiveness when combined with conventional T2-weighted imaging, with an inverse relationship between the apparent diffusion coefficient (ADC) map intensity and Gleason score [7]. DWI typically uses the echo-planar imaging (EPI) technique to decrease scan time. However, images acquired with EPI suffer from severe susceptibility artifact at the interfaces of tissue with air, blood, or fecal matter in the rectum. These artifacts are of particular importance because they present at the border of the rectum and the peripheral zone of the prostate, where 70% of prostate cancers are located [8].

In this work, we have utilized a reduced-field-of-view (rFOV) acquisition scheme for prostate DWI that employs a 90° 2D spatially-selective, echo-planar RF pulse to excite a limited extent in the phase field-of-view (FOV) direction [9]. This enables a higher spatial resolution to be achieved in the phase encoding direction than in conventional DWI with a shorter echo-train length, and without obvious aliasing artifacts. The reduced echo-train length can potentially reduce prostate image distortions induced by magnetic-susceptibility differences within the FOV [9]. Additionally, this pulse is designed so that the excited fat profile and the excited water profile do not overlap, so that only the on-resonance water profile can be selected by the subsequent refocusing pulse. This could potentially provide a robust method of periprostatic fat suppression in prostate DWI images [9].

The aim of this study was to determine if image distortion is less in prostate ADC maps generated from the rFOV technique than from a conventional DWI sequence (CONV) and to determine if the rFOV ADC contrast between tumors and healthy-appearing tissue within subjects is as high as or better than that of the CONV sequence.

2. Materials and Methods

2.1 Subjects

This prospective study was approved by our institutional review board and was compliant with the Health Insurance Portability and Accountability Act. Written, informed consent was obtained from all participants. Fifty patients receiving MR examinations of the prostate were studied between September of 2011 and January of 2013. Patients presented with suspected prostate cancer, as indicated by either elevated levels of serum prostate-specific antigen (PSA) (median=5, range 0.10–291), biopsy-proven prostate cancer, or both. The patients' mean age was 64.2 years, ranging from 47 to 81 years old. Two patients had undergone a partial radical prostatectomy, two patients had undergone hormone therapies, two patients had received external beam radiation therapy (EBRT), four patients had radiation seed implants, and one patient had received hormone therapy and EBRT. Data from the eleven patients having undergone any form of treatment were not used in assessment of contrast; however these data were included in visual and quantitative assessments of distortion.

Figure 1 shows a categorization of this study by patient group. Thirty-nine of the fifty patients studied were untreated and considered for inclusion in the study of contrast. Of these patients, ten were scanned with inconsistent MR parameters during initial trials of this study and were not considered for the studies of ADC values. The ADC value in presumed healthy peripheral zone tissue was assessed in the resulting twenty-nine patients. Within this group of twenty-nine patients, twelve had no positive biopsy on record. The seventeen remaining patients' data were used to calculate the contrast between tumor and healthy tissue for both CONV and rFOV sequences. Fourteen of these patients exhibited a Gleason score of 3+3. One patient each presented with Gleason scores of 3+4, 3+5, and 4+3.

2.2 MR imaging

All images were acquired using a 3T MR scanner (GE Healthcare, Waukesha, WI, USA) equipped with an eight-channel phased-array for the pelvis and an endorectal coil encased in a balloon probe (Bayer Healthcare, Warrendale, Pa, USA). A perfluorocarbon compound (3M, St. Paul, MN, USA) was used to inflate the balloon probe to reduce artifacts due to susceptibility [10].

Anatomic imaging was provided by oblique axial T2-weighted images (512×512, TR/TE=6350/103 ms). CONV (128×128, FOV=24cm × 24cm, NEX=4, TR/TE=4000/78–90ms, 2:44 minutes) and rFOV (128×64, FOV=18cm × 9cm (n=37) or 24cm × 12cm (n=13), NEX=6, TR/TE=4000/78–90ms, 2:52 minutes) DWI sequences were acquired using a 2D single-shot EPI (ss-EPI) spin-echo sequence with receiver bandwidth = 250kHz, b = 600 and 0 s/mm^2, and 3mm slices (n=37) or greater than 3mm slices (n=13). Parallel imaging was used in the CONV sequence, with an acceleration factor of 2. The rFOV acquisition employed a 2D spatially-selective echo-planar RF pulse in place of conventional excitation in the ss-EPI sequence. The RF envelope of the 2D echo-planar pulse (~18 ms duration) is minimum phase by design so the echo time occurs toward the end of the pulse. Because of this, and the fact that the spacing between the 90° pulse and the following 180° pulse is dominated by the diffusion weighting time, the RF pulse did not increase the echo time

compared to the conventional sequence. The time-bandwidth of the RF envelope (slice direction) was relatively small, therefore the slice dephasing from the non-linear phase excitation was relatively benign. The TE varied among patients due to changes in obliquity of the prostate and therefore, the scan prescription. The phase-encoding direction, and consequently the reduced-FOV axis for the rFOV DWI scan, was in the oblique anterior-posterior direction. The DWI images were obtained with slice locations and obliquity identical to the oblique axial T2-weighted images. Thirteen patients were scanned with the rFOV sequence acquired with FOV = 24cm × 12cm and the slice thickness greater than 3 mm during initial testing. These patients' data, acquired with inconsistent MR parameters, were used in the quantitative and visual assessments of distortion. Although ten of the thirteen patients presented with radiologist-identified tumor regions, the data were not used in the study of contrast to avoid any bias due to different partial voluming effects.

Under the assumption that prostate tissue is isotropic, ADC maps were computed from the combined DWI and T2-weighted reference images using Eq. (1).

$$ADC = \frac{-1}{\mathrm{b}} \ln \frac{\mathrm{S_{gm}}}{\mathrm{S_0}} \quad \text{Eq.(1)}$$

where b represents the b-value used in the diffusion-weighted acquisition reflecting the gradient strength and duration, S_{gm} is the geometric mean of the signal intensity over the six gradient directions, and S_0 is the signal intensity of the T2-weighted image in which there are no diffusion gradients.

2.3 Image Processing

The incidence and severity of visually assessed distortion was characterized by changes in the contour of the prostate adjacent to the rectal wall. The rFOV and CONV ADC maps were scored 0 for no distortion, and 1–4 for increasing distortion. A distortion score of 0 reflects no visible change in the boundary between prostate and rectum in comparison to a T2-weighted image. A distortion score of 1 reflects slight disturbances in the boundary region, whereas a distortion score of 2 is appropriate for more extensive disturbances in the boundary, or specific regions of high susceptibility artifact. A distortion score of 3 denotes a consistently distorted prostatic boundary, with some areas in the prostate unusable due to susceptibility artifact, and a distortion score of 4 is used to describe a prostate image that is entirely unusable due to susceptibility artifact. Examples of each distortion score are shown in Figure 2. All distortion scores were assigned by three independent observers to control for inter-observer variability. T2-weighted oblique axial images were used as a reference of no distortion.

A quantitative method of measuring distortion was also performed by comparing the radii of circles that reflect rectal wall curvature adjacent to the prostate. The inflated endorectal probe creates a reliably circular rectum on oblique axial images, and deviation from the circular pattern is a typical sign of susceptibility-induced distortion. On CONV, rFOV, and T2-weighted images, the radius of the largest circle tracing the rectum adjacent to the prostate, and without covering the rectal wall, was recorded on three slices. An example of this process is shown in Figure 3. These three selected slices were equally spaced throughout

the prostate—in the base, midgland, and apex—and matched in location among image types. The percent difference of the rectal wall radius on the CONV and rFOV ADC maps from the corresponding radius on the T2-weighted image was calculated for each of the three slices. These values were averaged within each patient to create a quantitative distortion measure of each DWI sequence for each patient.

Regions of interest (ROIs) were placed in areas of presumed healthy peripheral zone tissue in the group evaluated for assessment of healthy ADC values (see Figure 1). ROIs were also placed in areas of reduced ADC corresponding to suspected tumor regions and in areas of presumed healthy contralateral tissue in each patient included in the study of contrast (see Figure 1). Suspected tumor regions were identified as regions of both positive biopsy findings and radiologist-identified tumor in the MR exam. For patients with more than one biopsy-proven tumor region, the most aggressive tumor region was used to calculate contrast. For a given patient, all tumor ROIs and control ROIs were the same size within one pixel, and ranged between 0.143 and 0.642 cm^2. ROIs for all patients were drawn by a single researcher to avoid inter-observer variability. Tumor contrast was calculated using Eq. (2).

$$Contrast = \left| \frac{ADC_{\text{tumor}} - ADC_{\text{healthy}}}{ADC_{\text{healthy}}} \right| \quad \text{Eq.(2)}$$

Statistical analyses were performed using JMP V10 software (SAS Institute, Cary, NC, USA). A Wilcoxon Signed-Rank Test was performed to assess significant differences between CONV and rFOV distortion scores for each observer. The difference in distortion scores between CONV and rFOV images for each patient was compared among the three observers using a Kruskal-Wallis Rank Sum Test. Differences in rectal curvature for a quantitative distortion assessment were tested by student's t-tests. Differences in tumor, healthy tissue, and tumor-to-healthy-tissue contrast in CONV and rFOV scans were also tested for significance using student's t-tests. Tests for normalcy were done using a Shapiro-Wilk Test for goodness of fit.

3. Results

Forty-nine of the fifty patients (98%) assessed showed rectal wall distortion interfering with the peripheral zone of the prostate on either the CONV or rFOV sequence by at least one observer. Examples of each distortion score are shown in Figure 2. Distortion scores were significantly reduced with the rFOV sequence ($p<0.012$ Wilcoxon Signed-Rank Tests, $n=50$). Significance and average difference between sequences scored by each observer are shown in Table 1. The measured difference between CONV and rFOV distortion for a given patient did not vary significantly among observers ($p=0.99$, Kruskal-Wallis Rank Sum Test, $n=50$ counts per group, 3 groups).

The quantitative measure of distortion—the average percent difference in rectal wall radii between the ADC maps and the T2-weighted images—also demonstrated lower distortion with the rFOV sequence than the CONV sequence. The average percent difference in rectal

wall radii compared to T2-weighted reference images was significantly lower for rFOV ADC maps (26 ± 10%) than for CONV ADC maps (34 ± 13%) ($p<0.011$, n=50, student's t-test).

A typical distortion case (Figure 4) shows a patient whose rectal wall signal has merged with the medial prostate peripheral zone signal, drastically distorting the entire prostate border and the periphery of the tumor on the CONV ADC in this region. This patient had an average distortion score of 2.67 on CONV ADC and 1.33 on rFOV ADC and a percent difference of rectal wall radii of 50.8% on CONV ADC and 21.8% on rFOV ADC. A second example case (Figure 5) shows either blood or fecal matter as dark lobules in the rectal wall with localized susceptibility artifact on the CONV ADC map demonstrating an average distortion score of 2.33. These distortions are greatly reduced on the rFOV ADC map, with an average distortion score of 1. The quantitative distortion measure yielded 20.1% percent difference on the CONV ADC map and 14.8% on the rFOV ADC map.

All reported ADC values (measured by units of $10^{-3}mm^2/s$) and ADC contrast values were normally distributed across the studied population (Shapiro-Wilk Tests). The average ADC in healthy tissue for the twenty-nine untreated patients was 1.616±0.399 for the CONV and 1.733±0.223 for the rFOV, which were not significantly different, $p=0.754$.

For the seventeen patients included in the study of tumor contrast, the rFOV sequence provided significantly higher absolute value of the contrast between tumor and healthy tissue (average contrast = 44.0%) than the CONV sequence (average contrast = 35.9%) ($p<0.0012$, n=17, student's t-test). ADC values for tumor and healthy tissues with corresponding contrast values are listed in Table 2 for this group of patients. For the CONV and rFOV sequences, the ADC values in the healthy tissue of the untreated patients presenting with tumor were not significantly different ($p<0.9782$, n=17, student's t-test). However, the intensities of the tumor regions in the rFOV ADC maps had a trend to be lower than the corresponding tumor regions in the CONV ADC maps ($p<0.0854$, n=17, student's t-test).

4. Discussion

This study demonstrated that an alternate DWI acquisition scheme, based on using a pulse sequence with reduced-FOV excitation, provided significantly less image distortion and significantly improved contrast between tumor and healthy tissue ADC compared to a conventional DWI sequence acquired with a full phase-direction FOV. To the best of our knowledge, this is the first study to compare either susceptibility-related distortion or tumor contrast in prostate DWI utilizing conventional- and reduced-FOV DWI acquired in the same exam.

It must be noted that the patient population in this study was enrolled regardless of Gleason score, and as a result does not adequately represent a range of tumor aggressiveness. Regardless, the CONV ADC values measured in this study in tumor (mean = $1.00 \pm 0.52\times10^{-3}$ mm^2/s) and healthy tissue (mean = $1.61 \pm 0.40\times10^{-3}$ mm^2/s) were similar to those from other studies, which had healthy values ranging from $1.59 \pm 0.04\times10^{-3}$ mm^2/s to

$1.75 \pm 0.23 \times 10^{-3}$ mm^2/s [3,5] and tumor values for Gleason Score = 6 disease ranging from $0.86 \pm 0.04 \times 10^{-3}$ mm^2/s to $1.3 \pm 0.30 \times 10^{-3}$ mm^2/s [11–12]. Absolute contrast measures between tumor ADC and healthy tissue ADC were also similar to the values from the literature, which were estimated to be in the range of 28% to 40% [4,7].

Because the implementation of the rFOV technique in this study allows a higher image resolution compared to the CONV sequence while maintaining clinically-applicable scan times, the technique also decreases partial voluming effects in heterogeneous tissue. The reduced partial volumning and the reduced distortion near tissue interfaces may be partially responsible for the observed significant increase in image contrast between tumor and healthy tissue in the rFOV sequence in comparison to the CONV sequence.

Other acquisition schemes that reduce the number of phase encoding steps could result in reduced distortion for EPI DWI. However, such methods result in either aliasing in the image, or require a very large FOV to span the body, resulting in poor spatial resolution. The sequence described in this work uses a pulse sequence incorporating a rectangularly-selective excitation, which enables us to attain a FOV smaller than the body size in the phase-encoding direction, thus achieving high spatial resolution.

Recently, there have been several published works using various rectangularly-selective DWI approaches to improve spatial resolution or increase image quality for optic nerve, spine, and prostate imaging [13–16], which are fundamentally different from the rFOV sequence tested in this study due to the usage of non-coplanar RF pulses. One such modified DWI acquisition technique was recently evaluated to increase the quality of prostate DWI for the purposes of tractography [14]. This technique is the zonal oblique multi-slice diffusion tensor imaging (ZOOM) DTI sequence, which uses tilted non-coplanar RF pulses to refocus spins contained in the imaging slice. This sequence was developed to perform DWI in the presence of large volumes of fat and unpredictable motion and has demonstrated significant improvement in DWI images of the optic nerve [13]. A drawback of the technique is that the non-coplanar pulses leave residual signal in the imaging plane adjacent to the imaged slice. For multi-slice imaging, utilizing this method requires either increasing the gap between slices to avoid unwanted excitation in the imaging plane, or increasing scan time to ensure imaged tissue is fully relaxed before acquiring each slice, making this method most effective in imaging one-dimensional anatomy, as in the optic nerve. The evaluation in the prostate utilized a smaller FOV and higher spatial resolution than the conventional diffusion technique. ZOOM DTI provided a greater number of fibers detected and more homogeneous fat saturation but did not result in a reduction in prostate image distortions in the small patient population. In contrast, in this study we demonstrate a significant reduction in prostate DWI image distortion with the rFOV technique compared to the CONV sequence.

Another, similar technique to reduce the FOV in MR of the prostate using outer volume suppression has been presented by Reischauer et al. [15]. This research measured ADC performance for prostate cancer detection showing high accuracy (73.5%), specificity (75.2%), and sensitivity (70.4%) in comparison to biopsy, but did not compare the ADC obtained from the novel technique with ADC from the conventional technique to assess the

impact on distortion. As both this study and ours reduce the number of phase encoding steps acquired, both are apt to reduce susceptibility artifact in the images, and their study did report attaining high quality images. However, the outer volume suppression method excites tissue adjacent to the imaged slice similar to the ZOOM DTI method, again requiring either increased slice gap or wait time for relaxation. While likely similar in reducing distortion artifact, our study used a different technique which does not excite adjacent tissue (2D, echo-planar RF refocusing pulse [9]) to achieve the reduced-FOV enabling multi-slice imaging without requiring increased scan time or slice gap. However we did not perform a direct comparison to this technique and thus cannot compare the image quality.

Additionally, the pulse sequence used in our research study has been previously demonstrated to enable high spatial resolution and qualitatively increase image quality in breast DWI [17] and pancreatic DWI [18]. These studies demonstrated that the mean ADC of tumor regions was not significantly different between rFOV and CONV DWI. However, the minimum ADC value of a tumor region was found to be significantly lower in the rFOV sequence in the breast study [17]. These findings are consistent with our results that demonstrated qualitatively and quantitatively increased image quality and non-significant differences between the ADC values of the CONV and rFOV sequences with a trend toward lower tumor ADC values for rFOV than the CONV sequence. The pancreatic study [18] found no difference between ADC values in CONV and rFOV DWI images, however the sequence was designed to maximize the image quality in favor of increasing contrast. Although these studies represent potential for rFOV DWI in a variety of organs, our study investigated the unique scenario of imaging a thin band of tissue of interest (the peripheral zone) adjacent to tissue with potentially drastically different magnetic susceptibility (air, fecal matter, or blood in the rectum), prone to severe distortion artifacts.

In spite of the sharp excitation profile in the phase encoding direction from the high time-bandwidth 2D RF pulse used in the rFOV sequence [9], in our particular application, signal in the transition band from the very high fluid signal along the rectal wall—such as a perineal hernia—can cause serious wrapping artifact. There is risk of such signal wrapping into the central gland of patients with very large prostates. This is particularly limiting to patients who suffer from benign prostatic hyperplasia, which increases PSA and prostate size, typically leading to clinical testing for prostate cancer staging. Encoding a slightly larger FOV than the excited FOV extent or adding a saturation band to the oblique posterior of the prostate can prevent this artifact.

One limitation of this study is the measures were user dependent in scoring the distortion, in identifying corresponding slices, and in visually matching circles to the rectal wall. However, the changes in visual scores between the CONV and the rFOV sequences were very similar among the three readers. Also, both the visual scoring and the quantitative measures of rectal wall distortion yielded similarly significant reduction in distortion with the rFOV sequence compared to the CONV sequence. These results lend confidence to our conclusion that the rFOV sequence results in less image distortion on ADC maps than the CONV sequence.

Another limitation of this study is the use of a single, non-zero b-value in all patients with comparison to a b=0 image. Our ADC values may differ from those obtained using a non-zero reference image. Although there is no consensus on the optimal b-value for prostate cancer detection, in addition to the moderate b-value we used (b=600), studies have shown relevance for high-b-value acquisition for detection of prostate cancer [19–20]. At higher b-values, the rFOV DWI acquisition would require increased averaging to boost the SNR, increasing scan time. Due to scan time constraints in the present study, rFOV DWI at higher b values was not acquired in this work but will be explored in the future.

Despite the limited scope of our study, the distortion due to susceptibility artifact was significantly lower in the rFOV sequence than in the comparable CONV sequence. Additionally, the rFOV technique employed has been shown to increase contrast between biopsy-proven, radiologist-identified tumor regions and healthy contralateral tissue. This is particularly important, as the ADC map intensity is known to correlate with tumor grade in prostate cancer [7]. Increasing tumor contrast may increase the value of using the ADC map for both detecting prostate cancer and assessing its grade.

5. Conclusion

In conclusion, the rFOV sequence yielded significantly decreased rectal wall susceptibility artifact and provided significantly higher contrast in ADC value between tumor and healthy tissue as compared to the CONV sequence without significantly increasing scan time. This technique shows great promise for improving DWI quality, thereby potentially improving the detection of prostate cancer by MRI.

References

1. Cancer Facts and Figures 2013. Atlanta, GA: American Cancer Society; 2013. Available from http://www.cancer.org/research/cancerfactsfigures/cancerfactsfigures/cancer-facts-figures-2013
2. Kurhanewicz J, Vigneron D, Carroll P, Coakley F. Multiparametric magnetic resonance imaging in prostate cancer: present and future. Curr Opin Urol. 2008; 18(1):71–77. [PubMed: 18090494]
3. Mazaheri Y, Vargas H, Nyman G, Shukla-Dave A, Akin O, Hricak H. Diffusion-weighted MRI of the prostate at 3.0T: Comparison of endorectal coil (ERC) MRI and phased-array coil (PAC) MRI - The impact of SNR on ADC measurement. Euro J Rad. 2013; 82:515–520.
4. Gibbs P, Pickles MD, Turnbull LW. Diffusion imaging of the prostate at 3.0 tesla. Invest Radiol. 2006; 41(2):185–188. [PubMed: 16428991]
5. Turkbey B, Pinto PA, Choyke PL. Imaging techniques for prostate cancer: implications for focal therapy. Nat Rev Urol. 2009; 6(4):191–203. [PubMed: 19352394]
6. Kim CK, Park BK, Lee HM, Kwon GY. Value of diffusion-weighted imaging for the prediction of prostate cancer location at 3T using a phased-array coil: preliminary results. Invest Radiol. 2007; 42(12):842–847. [PubMed: 18007156]
7. Vargas HA, Akin O, Franiel T, et al. Diffusion-weighted endorectal MR imaging at 3 T for prostate cancer: tumor detection and assessment of aggressiveness. Radiology. 2011; 259(3):775–784. [PubMed: 21436085]
8. Rickards D. Transrectal ultrasound 1992. Br J Urol. 1992; 69(5):449–455. [PubMed: 1623369]
9. Saritas EU, Cunningham CH, Lee JH, Han ET, Nishimura DG. DWI of the spinal cord with reduced FOV single-shot EPI. Magn Reson Med. 2008; 60(2):468–473. [PubMed: 18666126]
10. Noworolski SM, Crane JC, Vigneron DB, Kurhanewicz J. A clinical comparison of rigid and inflatable endorectal-coil probes for MRI and 3D MR spectroscopic imaging (MRSI) of the prostate. J Magn Reson Imaging. 2008; 27(5):1077–1082. [PubMed: 18407539]

11. Hambrock T, Somford DM, Huisman HJ, et al. Relationship between Apparent Diffusion Coefficients at 3.0-T MR Imaging and Gleason Grade in Peripheral Zone Prostate Cancer. Radiology. 2011; 259(2):453–461. [PubMed: 21502392]
12. Woodfield CA, Tung GA, Grand DJ, Pezzullo JA, Machan JT, Renzulli JF 2nd. Diffusion-weighted MRI of peripheral zone prostate cancer: comparison of tumor apparent diffusion coefficient with Gleason score and percentage of tumor on core biopsy. AJR Am J Roentgenol. 2010; 194(4):W316–W322. [PubMed: 20308476]
13. Wang MY, Qi PH, Shi DP. Diffusion tensor imaging of the optic nerve in subacute anterior ischemic optic neuropathy at 3T. AJNR Am J Neuroradiol. 2011; 32(7):1188–1194. [PubMed: 21700789]
14. Takahashi YU S, Kitajima K, Okuaki T, Sugimura K. Tractography of the Neurovascular Bundles of the Prostate with Zoom DTI Technique: Preliminary Report. ISMRM. Salt Lake City. 2013 (abstract 1780).
15. Reischauer C, Wilm BJ, Froehlich JM, et al. High-resolution diffusion tensor imaging of prostate cancer using a reduced FOV technique. Eur J Radiol. 2011; 80(2):e34–e41. [PubMed: 20638208]
16. Jeong EK, Kim SE, Guo J, Kholmovski EG, Parker DL. High-resolution DTI with 2D interleaved multislice reduced FOV single-shot diffusion-weighted EPI (2D ss-rFOV-DWEPI). Magn Reson Med. 2005; 54(6):1575–1579. [PubMed: 16254946]
17. Singer L, Wilmes LJ, Saritas EU, et al. High-resolution diffusion-weighted magnetic resonance imaging in patients with locally advanced breast cancer. Acad Radiol. 2012; 19(5):526–534. [PubMed: 22197382]
18. Ma C, Li Y, Pan C, et al. High resolution diffusion weighted magnetic resonance imaging of the pancreas using reduced field of view single-shot echo-planar imaging at 3 T. Magn Reson Imaging. 2014; 32(125–131)
19. Kitajima K, Kaji Y, Kuroda K, Sugimura K. High b-value diffusion-weighted imaging in normal and malignant peripheral zone tissue of the prostate: effect of signal-to-noise ratio. Magn Reson Med Sci. 2008; 7(2):93–99. [PubMed: 18603841]
20. Kim CK, Park BK, Kim B. High-b-value diffusion-weighted imaging at 3 T to detect prostate cancer: comparisons between b values of 1,000 and 2,000 s/mm2. AJR Am J Roentgenol. 2010; 194(1):W33–W37. [PubMed: 20028888]

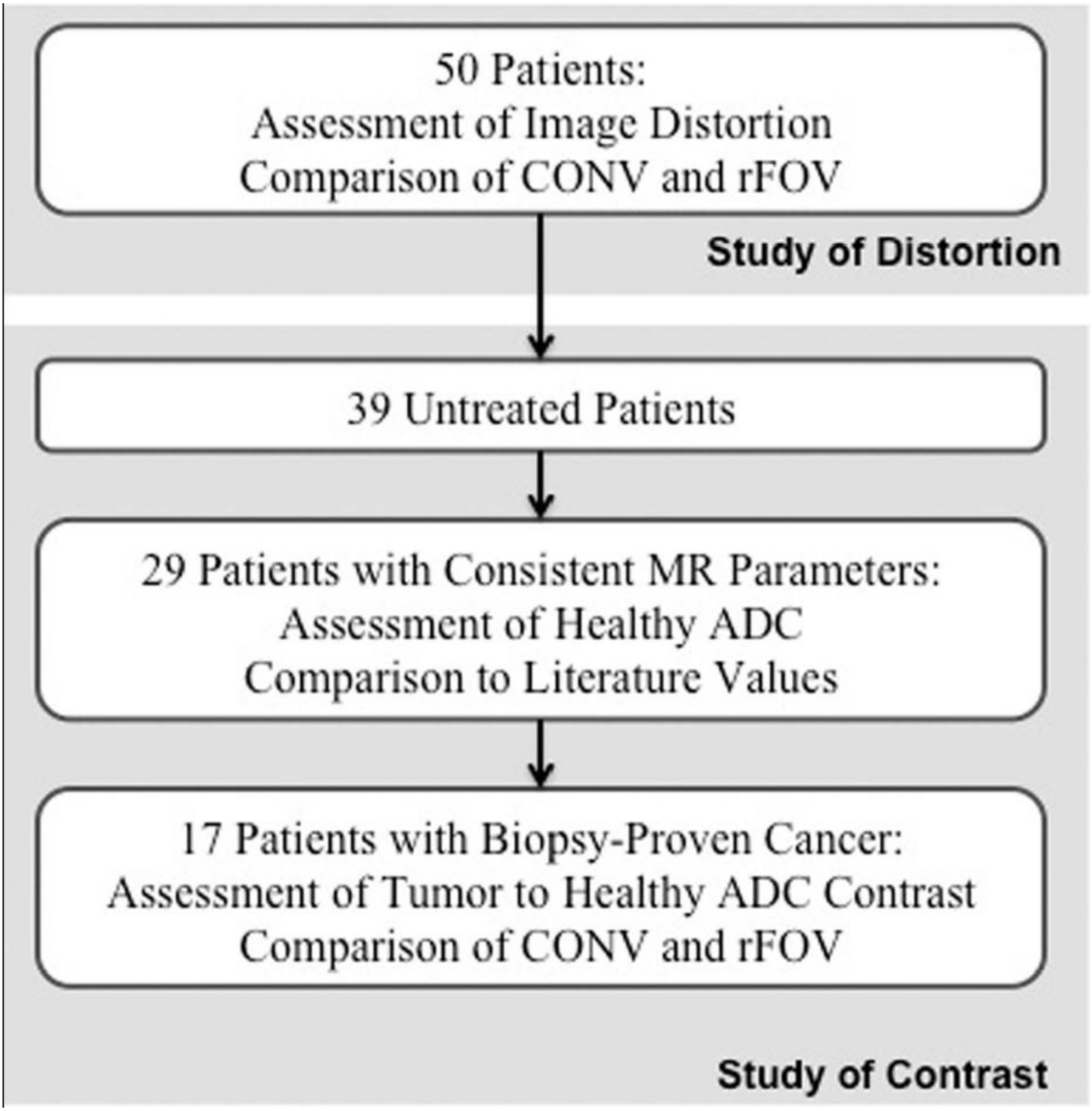

Figure 1.
Grouping of patient population by studies of prostate distortion at the rectal border and ADC contrast between tumor and healthy tissue.

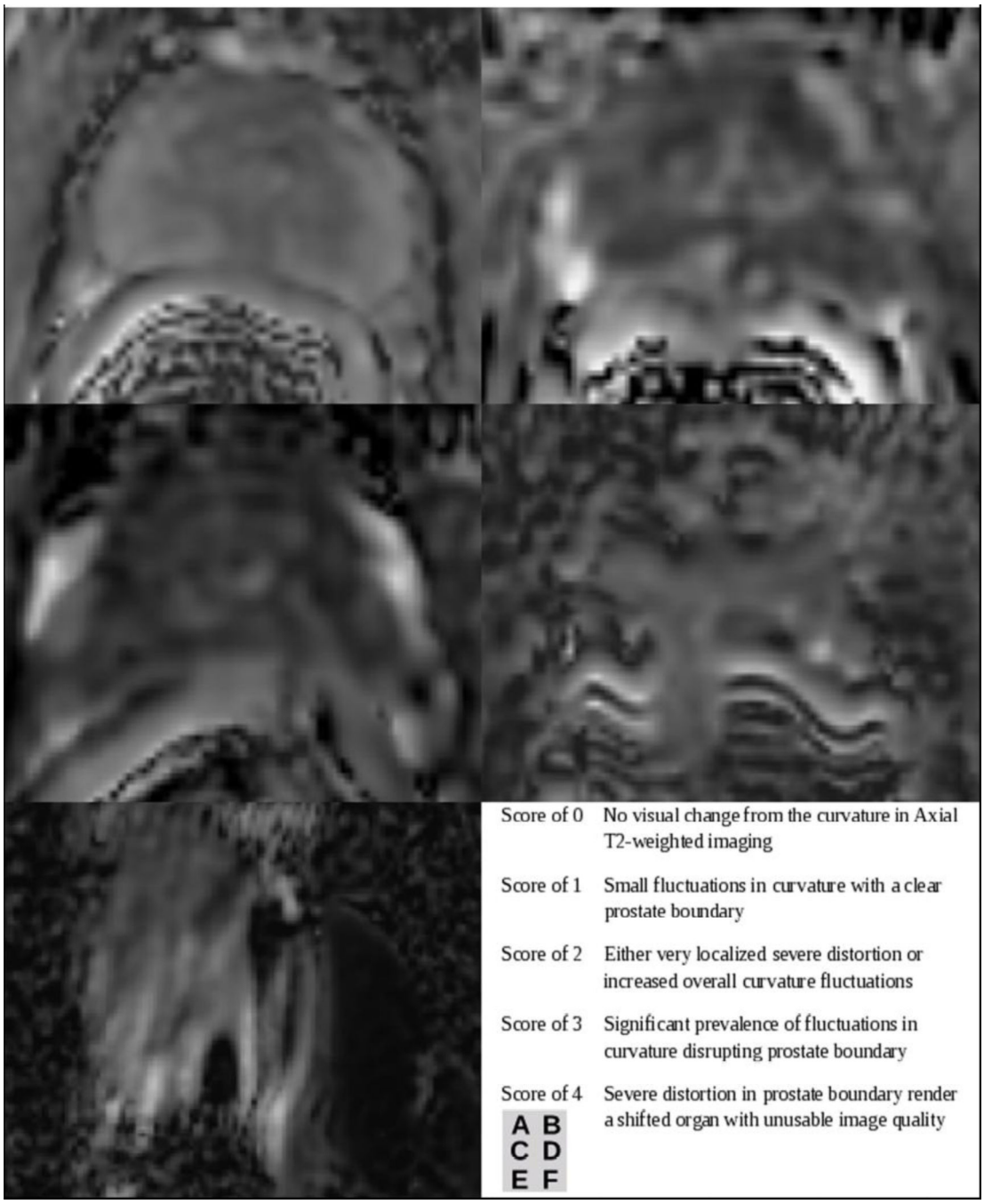

Figure 2.

Distortion scores from sample patients showing A) score of 0, B) score of 1, C) score of 2, D) score of 3, E) score of 4, and F) a guideline of visual score interpretation. Please note that E) contains artifact that has rotated the prostate signal, rendering spatial localization unusable.

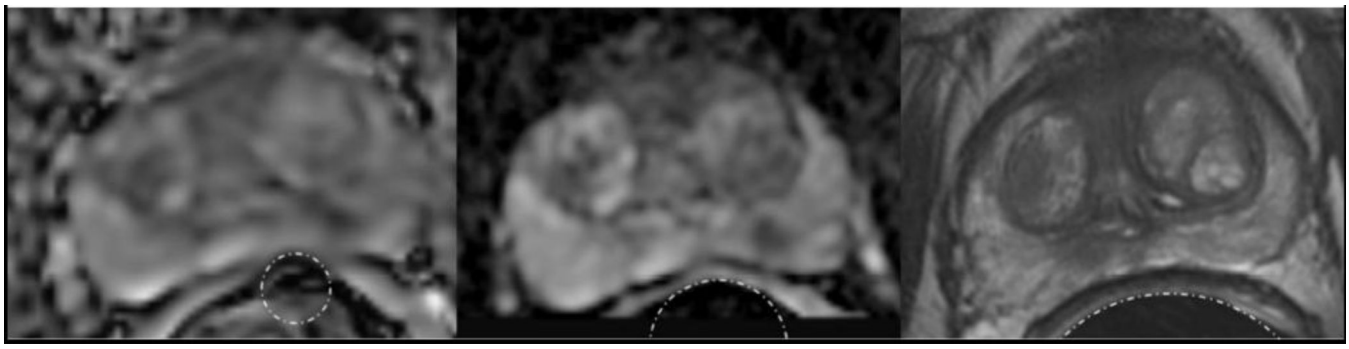

Figure 3.

Oblique axial images of (a) CONV ADC map, (b) rFOV ADC map, and (c) T2-weighted image for a patient with overlaid circular regions of interest to quantitatively measure the difference in rectal curvature due to image distortion. The average percent difference from T2-weighted image rectal wall radius over three representative slices for this patient was 53.6% on CONV and 31.5% on rFOV. This is a patient with a positive biopsy showing Gleason 4+3, on active surveillance at the time of this scan.

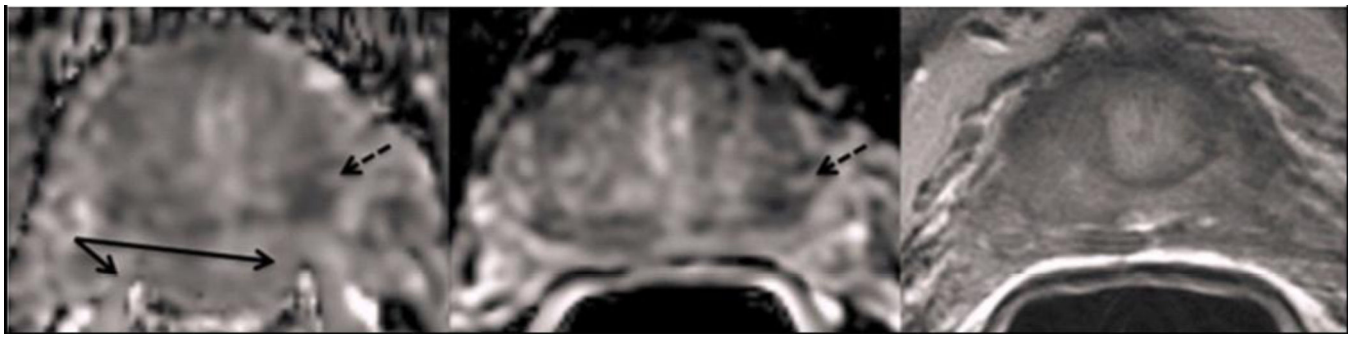

Figure 4.

Oblique axial images of (a) CONV ADC map, (b) rFOV ADC map, and (c) T2-weighted image for a patient with a visible tumor in the left peripheral zone (dashed arrows). The boundary of the rectum and peripheral zone (solid arrow) is distorted in the CONV image, less so in the rFOV image, and not at all in the T2-weighted image. This is a patient with a negative biopsy and recently elevated PSA of 2.0, on active surveillance at the time of this scan.

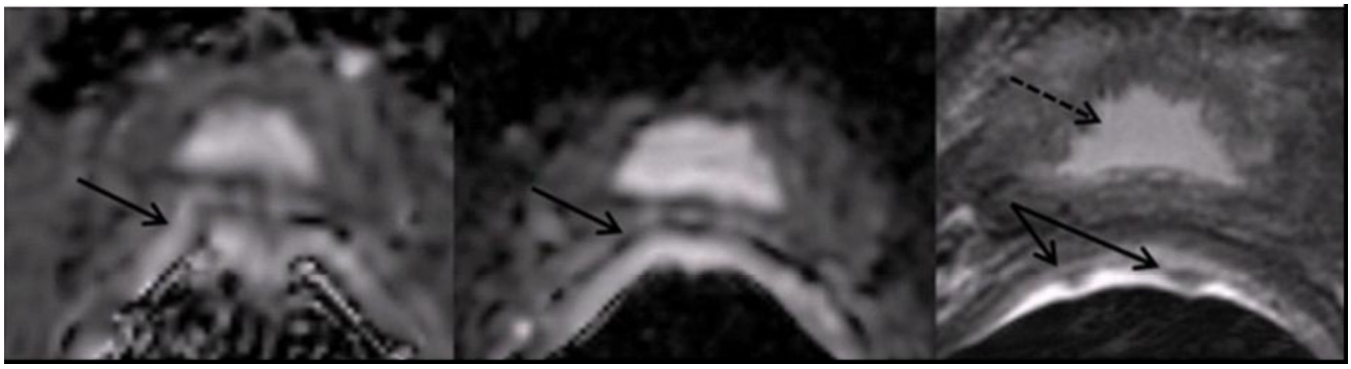

Figure 5.
Oblique axial images of (a) CONV ADC map (b) rFOV ADC map and (c) T2-weighted image at the base of the prostate near the bladder (dashed arrow) for a patient with blood or fecal artifact visible at the rectum/peripheral zone interface (solid arrows). This is a patient with a positive biopsy showing Gleason Score 3+3, on active surveillance at the time of this scan.

Table 1

Distortion Scoring by Observer

Observer	rFOV Improvement Significance	CONV - rFOV Difference (0–4 Scale) (Average ± SD)
1	p<0.0063	0.56±0.68
2	p<0.0117	0.48±0.61
3	p<0.0010	0.52±0.65

Wilcoxon Signed-Rank Tests for difference in distortion scoring among patients show a significant decrease in observed distortion in ADC maps created from the reduced-Field-of-View (rFOV) sequence compared to the conventional (CONV) sequence for each observer (n=50). The average decrease in distortion score is similar for all observers, p=0.99, Kruskal-Wallis Rank Sum Test, SD = standard deviation.

Table 2

ADC Values in Tumor and Healthy Tissue

Case	Tumor ADC	Healthy Tissue ADC	Contrast (%)
CONV	1.022±.185	1.620±.231	35.9±13.2*
rFOV	0.952±.180	1.731±.230	44.0±13.3*

Conventional sequence (CONV) and reduced-Field-Of-View sequence (rFOV) apparent diffusion coefficient (ADC) values [$\times 10^{-3} mm^2/s$] and contrast [%] for untreated patients with identified tumor (n=17). ADC values show no statistical difference between healthy tissue in tested sequences (p=0.978) and a trend towards lower ADC values in tumor regions using rFOV (p<0.0854).

*Magnitude of tumor contrast is significantly higher in the rFOV sequence than in the CONV sequence (p<0.0012).